ARMY RESEARCH LABORATORY

Dissipative Particle Dynamics at Isothermal Conditions Using Shardlow-Like Splitting Algorithms

by John K. Brennan and Martin Lísal

ARL-TR-6582 **September 2013**

NOTICES

Disclaimers

The findings in this report are not to be construed as an official Department of the Army position unless so designated by other authorized documents.

Citation of manufacturer's or trade names does not constitute an official endorsement or approval of the use thereof.

Destroy this report when it is no longer needed. Do not return it to the originator.

Army Research Laboratory
Aberdeen Proving Ground, MD 21005-5066

ARL-TR-6582 **September 2013**

Dissipative Particle Dynamics at Isothermal Conditions Using Shardlow-Like Splitting Algorithms

John K. Brennan
Weapons and Materials Research Directorate, ARL

Martin Lísal
Institute of Chemical Process Fundamentals of the ASCR
and
J. E. Purkinje University

REPORT DOCUMENTATION PAGE	Form Approved OMB No. 0704-0188

1. REPORT DATE *(DD-MM-YYYY)*	2. REPORT TYPE	3. DATES COVERED (From - To)
September 2013	Final	April 2010–January 2013

4. TITLE AND SUBTITLE
Dissipative Particle Dynamics at Isothermal Conditions Using Shardlow-Like Splitting Algorithms

5a. CONTRACT NUMBER

5b. GRANT NUMBER

5c. PROGRAM ELEMENT NUMBER

6. AUTHOR(S)
John K. Brennan and Martin Lísal*

5d. PROJECT NUMBER

5e. TASK NUMBER

5f. WORK UNIT NUMBER

7. PERFORMING ORGANIZATION NAME(S) AND ADDRESS(ES)
U.S. Army Research Laboratory
ATTN: RDRL-WML-B
Aberdeen Proving Ground, MD 21005-066

8. PERFORMING ORGANIZATION REPORT NUMBER
ARL-TR-6582

9. SPONSORING/MONITORING AGENCY NAME(S) AND ADDRESS(ES)

10. SPONSOR/MONITOR'S ACRONYM(S)

11. SPONSOR/MONITOR'S REPORT NUMBER(S)

12. DISTRIBUTION/AVAILABILITY STATEMENT
Approved for public release; distribution is unlimited.

13. SUPPLEMENTARY NOTES
*Institute of Chemical Process Fundamentals of the ASCR and J. E. Purkinje University

14. ABSTRACT
A numerical integration scheme based upon the Shardlow-splitting algorithm (SSA) is presented for the constant-temperature dissipative particle dynamics method. The SSA is formulated for both a velocity-Verlet scheme and an implicit scheme, where the velocity-Verlet scheme consistently performed better. The original SSA formulated for systems of equal-mass particles has been extended to systems of unequal-mass particles. For completeness, the Fokker-Planck equation and derivation of the fluctuation-dissipation theorem are included.

15. SUBJECT TERMS
dissipative particle dynamics, modeling, simulation, Shardlow-splitting algorithm, isothermal

16. SECURITY CLASSIFICATION OF:			17. LIMITATION OF ABSTRACT	18. NUMBER OF PAGES	19a. NAME OF RESPONSIBLE PERSON
a. REPORT	b. ABSTRACT	c. THIS PAGE			John K. Brennan
Unclassified	Unclassified	Unclassified	UU	30	19b. TELEPHONE NUMBER (*Include area code*) 410-306-0678

Contents

List of Figures

Acknowledgments

The authors would like to thank Joshua D. Moore, Sergey Izvekov, and Betsy M. Rice (U.S. Army Research Laboratory) for insightful discussions. Martin Lísal acknowledges that this research was sponsored by the U.S. Army Research Laboratory and was accomplished under Cooperative Agreement Number W911NF-10-2-0039. The views and conclusions contained in this document are those of the authors and should not be interpreted as representing the official policies, either expressed or implied, of the U.S. Army Research Laboratory or the U.S. government. The U.S. government is authorized to reproduce and distribute reprints for government purposes notwithstanding any copyright notation herein. John K. Brennan acknowledges support in part by the Office of Naval Research and the Department of Defense High Performance Computing Modernization Program Software Application Institute for Multiscale Reactive Modeling of Insensitive Munitions.

INTENTIONALLY LEFT BLANK.

1. Introduction

Since its development almost 20 years ago, dissipative particle dynamics (DPD) (*1*, *2*) has become a robust tool for simulating soft condensed matter including polymers, surfactants, and colloids (see e.g., Brennan and Lísal [*3*] and references therein). Though often used to simulate polymer systems, DPD is now being applied in other areas such as biophysics (*4*) and shock physics (*5*). Moreover, DPD models have advanced beyond the typical purely repulsive models (e.g., references *6*–*9*), including augmentations that capture noncentral shear forces (*7, 10*).

When applying the DPD method, numerical integration of the equations-of-motion (EOM) is a key consideration, where the stochastic component requires special attention. Efficient and accurate integration schemes are required to maintain reasonable time step sizes, thus allowing for the simulation of mesoscale events. Moreover, the advent of conservative forces extending beyond purely-repulsive models that contain attractive character further supports the need for effective integration schemes. However, the integration is a nontrivial task due to the pairwise coupling of particles through the random and dissipative forces (*11*). Furthermore, self-consistent solutions are often necessary because the dissipative forces and the relative velocities of the particles are interdependent, where the considerable computational cost associated with this task has motivated the development of various integration schemes. Recent independent studies by Nikunen et al. (*11*) and Chaudhri and Lukes (*12*) assessed the quality and performance of several applicable integration schemes for constant-temperature DPD, specifically, the velocity-Verlet-based integrator (*13*), self-consistent Pagonabarraga-Hagen-Frenkel integrator (*14*), self-consistent velocity-Verlet integrator (*15, 16*), den Otter-Clarke integrator (*17*), first- and second-order Shardlow-splitting algorithms (SSAs) (*18*), and Lowe-Andersen integrator (*19*). Still other schemes are possible such as the Peters integrator (*20*) and a scheme similar to the SSA developed by Litvinov et al. (*21*) for highly dissipative smoothed-particle dynamics. Further, De Fabritiis et al. (*22*) developed numerical integrators for stochastic models using the Trotter expansion, and later applied the stochastic Trotter expansion to the constant-temperature DPD method (*23*). They tested the DPD-Trotter integration scheme on a DPD fluid and found accuracy comparable to the SSA but with a 10% speed-up. The consensus from all of these studies identified the SSA (*18*) as the best-performing approach.

The SSA decomposes the EOM into differential equations that correspond to the deterministic dynamics and the elementary stochastic differential equations that correspond to the stochastic dynamics. In the original SSA formulation, both types of differential equations are integrated via the velocity-Verlet algorithm (*18*), where the stochastic dynamics are additionally solved in an implicit manner that conserves linear momentum. Previously, the SSA had been applied only to the constant-temperature DPD method, while an SSA-inspired approach was implemented for a method in the spirit of the energy-conserving DPD method (*5*).

In this work, we modify the original SSA formulation for constant-temperature DPD systems of unequal-mass particles, followed by the development of an alternative algorithm to implicitly integrate the stochastic dynamics. The SSA is formulated for both a velocity-Verlet scheme and an implicit scheme, where the velocity-Verlet scheme consistently performed better. For completeness, the derivations of the Fokker-Planck equation (FPE) and the fluctuation-dissipation theorem (FDT) are included.

2. Formulation of DPD at Fixed Temperature Using Shardlow-Like Splitting Numerical Discretization

2.1 General Formulation of DPD

DPD particles are defined by a mass m_i, position $\mathbf{r}_i$, and momentum $\mathbf{p}_i$. The particles interact with each other via a pairwise force $\mathbf{F}_{ij}$ that is written as the sum of a conservative force $\mathbf{F}_{ij}^C$, dissipative force $\mathbf{F}_{ij}^D$, and random force $\mathbf{F}_{ij}^R$:

$$\mathbf{F}_{ij} = \mathbf{F}_{ij}^C + \mathbf{F}_{ij}^D + \mathbf{F}_{ij}^R . \tag{1}$$

$\mathbf{F}_{ij}^C$ is given as the negative derivative of a coarse-grain potential u_{ij}^{CG}, expressed as

$$\mathbf{F}_{ij}^C = -\frac{\mathrm{d}u_{ij}^{CG}}{\mathrm{d}r_{ij}}\frac{\mathbf{r}_{ij}}{r_{ij}} \tag{2}$$

where $\mathbf{r}_{ij} = \mathbf{r}_i - \mathbf{r}_j$ is the separation vector between particle i and particle j, and $r_{ij} = \left|\mathbf{r}_{ij}\right|$. The remaining two forces, $\mathbf{F}_{ij}^D$ and $\mathbf{F}_{ij}^R$, can be interpreted as a means to compensate for the degrees of freedom neglected by coarse graining. The conservative force is not specified by the DPD formulation and can be chosen to include any forces that are appropriate for a given application, including multibody interactions (e.g., references *6*, *8*, and *24*]). $\mathbf{F}_{ij}^D$ and $\mathbf{F}_{ij}^R$ are defined as

$$\mathbf{F}_{ij}^D = -\gamma_{ij}\omega^D\left(r_{ij}\right)\left(\frac{\mathbf{r}_{ij}}{r_{ij}}\cdot\mathbf{v}_{ij}\right)\frac{\mathbf{r}_{ij}}{r_{ij}} \tag{3}$$

and

$$\mathbf{F}_{ij}^R = \sigma_{ij}\omega^R\left(r_{ij}\right)W_{ij}\frac{\mathbf{r}_{ij}}{r_{ij}}, \tag{4}$$

where γ_{ij} and σ_{ij} are the friction coefficient and noise amplitude between particle i and particle j, respectively, and $\mathbf{v}_{ij} = \frac{\mathbf{p}_i}{m_i} - \frac{\mathbf{p}_j}{m_j}$ and W_{ij} are independent Wiener processes such that $W_{ij} = W_{ji}$. The weight functions $\omega^D(r)$ and $\omega^R(r)$ vanish for $r \geq r_c$, where r_c is the cutoff radius.

Note that $\mathbf{F}_{ij}^{C}$ is completely independent of $\mathbf{F}_{ij}^{D}$ and $\mathbf{F}_{ij}^{R}$, while $\mathbf{F}_{ij}^{D}$ and $\mathbf{F}_{ij}^{R}$ are not independent but rather are coupled through a fluctuation-dissipation relation. This coupling arises from the requirement that in the thermodynamic limit, the system samples the corresponding probability distribution. The necessary conditions can be derived using an FPE (*25, 26*), which is presented in this work.

2.2 Constant-Temperature DPD

For constant-temperature and constant-volume conditions, the evolution of DPD particles in time t is governed by the following EOM:

$$\mathrm{d}\mathbf{r}_i = \frac{\mathbf{p}_i}{m_i}\mathrm{d}t \qquad (i = 1,\ldots,N), \tag{5a}$$

$$\mathrm{d}\mathbf{p}_i = \sum_{j\neq i}\left(\mathbf{F}_{ij}^{C} + \mathbf{F}_{ij}^{D} + \mathbf{F}_{ij}^{R}\right)\mathrm{d}t \tag{5b}$$

where *N* is the total number of particles. This EOM set conserves total momentum $\mathbf{P} = \sum_i \mathbf{p}_i$ as a consequence of pairwise additivity of the conservative, dissipative, and random forces.

Español and Warren (*27*) showed that this system samples the canonical probability distribution and obeys the FDT if the following relations hold:

$$\begin{aligned} \sigma_{ij}^2 &= 2\gamma_{ij}k_{\mathrm{B}}T \\ \omega^D(r) &= \left[\omega^R(r)\right]^2 \end{aligned}, \tag{6}$$

where k_{B} is the Boltzmann constant and T is the temperature. For completeness, the FPE and an outline of the derivation of the FDT is provided in appendix A. $\omega^D(r)$ and $\omega^R(r)$ are typically chosen (*13*) as

$$\begin{aligned} \omega^D(r) = \left[\omega^R(r)\right]^2 &= \left(1-\frac{r}{r_c}\right)^2 \qquad (r < r_c) \\ &= 0 \qquad\qquad\qquad (r \geq r_c) \end{aligned}. \tag{7}$$

Note that the dependence of the random-force noise amplitude σ_{ij} on the temperature T can be physically interpreted as the system being in thermal contact with a heat reservoir.

2.2.1 Numerical Discretization

Next we review the first-order SSA (*18*). The original SSA was formulated for systems of particles with equal masses (*18*), while here we provide a formulation for systems with unequal masses. The basic idea of the SSA is the decomposition of the EOM (equations 5a and 5b) into

differential equations corresponding to the deterministic dynamics and elementary stochastic differential equations (SDEs) corresponding to the fluctuation-dissipation contributions. In the original SSA formulation, integration of both types of differential equations uses the velocity-Verlet algorithm (*28*).

For the constant-temperature DPD SSA formulation, the conservative terms consist of the following differential equations:

$$\mathrm{d}\mathbf{r}_i = \frac{\mathbf{p}_i}{m_i}\mathrm{d}t \qquad (i = 1,\ldots,N)\ , \tag{8a}$$

$$\mathrm{d}\mathbf{p}_i = \sum_{j\neq i}\mathbf{F}_{ij}^{C}\mathrm{d}t \tag{8b}$$

while the fluctuation-dissipation terms consist of the elementary SDEs:

$$\begin{aligned}\mathrm{d}\mathbf{p}_{i}^{i\text{-}j} &= -\gamma_{ij}\omega^{D}\left(\frac{\mathbf{r}_{ij}}{r_{ij}}\cdot\mathbf{v}_{ij}\right)\frac{\mathbf{r}_{ij}}{r_{ij}}\mathrm{d}t + \sigma_{ij}\omega^{R}\frac{\mathbf{r}_{ij}}{r_{ij}}\mathrm{d}W_{ij} \qquad \left(\text{for each } i<j\right)\\ \mathrm{d}\mathbf{p}_{j}^{i\text{-}j} &= -\mathrm{d}\mathbf{p}_{i}^{i\text{-}j}\end{aligned} \tag{9}$$

where the superscript $i-j$ indicates that the variation of momenta is considered for a pair of interacting particles i and j only, and $\mathrm{d}W_{ij} = \mathrm{d}W_{ji}$ are the increments of the Wiener processes. Note that equation 5b is recovered by adding $\sum_{j\neq i}\mathrm{d}\mathbf{p}_i^{i-j}$ to equation 8b.

Both the conservative and the fluctuation-dissipation terms can be solved using velocity-Verlet algorithms, where the SSA occurs in the following manner. First, denote the overall solution operator $\phi_{\Delta t}$ as the stochastic flow map for a time step Δt corresponding to the dynamics defined in equations 5a and b, and further denote $\phi_{\Delta t}^{C}$ and $\phi_{\Delta t;i,j}^{diss}$ $\left(1\le i<j\le N\right)$ as the solution operators or flow maps associated with equations 8a and b, and equation 9, respectively. (Stochastic flow maps are mathematical constructs that define solutions to SDEs, where the solution operators are performed in a successive manner. See Shardlow (*18*) and references therein for further discussion of stochastic flow maps and splitting methods for SDEs.) An approximation of $\phi_{\Delta t}$ for first-order splitting (*18*) can then be given as

$$\phi_{\Delta t} \cong \phi_{\Delta t;1,2}^{diss}\circ\phi_{\Delta t;1,3}^{diss}\circ\ldots\circ\phi_{\Delta t;i,j}^{diss}\circ\ldots\circ\phi_{\Delta t;N-2,N}^{diss}\circ\phi_{\Delta t;N-1,N}^{diss}\circ\phi_{\Delta t}^{C}\ , \tag{10}$$

where $\circ$ denotes a composition of operators.

For *each* fluctuation-dissipation term $\phi_{\Delta t;i,j}^{diss}$, momenta can be updated using the velocity-Verlet scheme (*18*):

$$\mathbf{p}_i\left(t+\frac{\Delta t}{2}\right)=\mathbf{p}_i(t)-\frac{\Delta t}{2}\gamma_{ij}\omega^D\left[\frac{\mathbf{r}_{ij}}{r_{ij}}\cdot\mathbf{v}_{ij}(t)\right]\frac{\mathbf{r}_{ij}}{r_{ij}}+\frac{\sqrt{\Delta t}}{2}\sigma_{ij}\omega^R\varsigma_{ij}\frac{\mathbf{r}_{ij}}{r_{ij}}, \tag{11a}$$

$$\mathbf{p}_j\left(t+\frac{\Delta t}{2}\right)=\mathbf{p}_j(t)+\frac{\Delta t}{2}\gamma_{ij}\omega^D\left[\frac{\mathbf{r}_{ij}}{r_{ij}}\cdot\mathbf{v}_{ij}(t)\right]\frac{\mathbf{r}_{ij}}{r_{ij}}-\frac{\sqrt{\Delta t}}{2}\sigma_{ij}\omega^R\varsigma_{ij}\frac{\mathbf{r}_{ij}}{r_{ij}}, \tag{11b}$$

$$\mathbf{p}_i(t+\Delta t)=\mathbf{p}_i\left(t+\frac{\Delta t}{2}\right)-\frac{\Delta t}{2}\gamma_{ij}\omega^D\left[\frac{\mathbf{r}_{ij}}{r_{ij}}\cdot\mathbf{v}_{ij}(t+\Delta t)\right]\frac{\mathbf{r}_{ij}}{r_{ij}}+\frac{\sqrt{\Delta t}}{2}\sigma_{ij}\omega^R\varsigma_{ij}\frac{\mathbf{r}_{ij}}{r_{ij}}, \tag{11c}$$

and

$$\mathbf{p}_j(t+\Delta t)=\mathbf{p}_j\left(t+\frac{\Delta t}{2}\right)+\frac{\Delta t}{2}\gamma_{ij}\omega^D\left[\frac{\mathbf{r}_{ij}}{r_{ij}}\cdot\mathbf{v}_{ij}(t+\Delta t)\right]\frac{\mathbf{r}_{ij}}{r_{ij}}-\frac{\sqrt{\Delta t}}{2}\sigma_{ij}\omega^R\varsigma_{ij}\frac{\mathbf{r}_{ij}}{r_{ij}}, \tag{11d}$$

where the superscript $i-j$ has been omitted for notational simplicity, and $\varsigma_{ij}=\varsigma_{ji}$ is a Gaussian random number with zero mean and unit variance that is chosen independently for each pair of interacting particles. (The use of $\sqrt{\Delta t}$ rather than Δt, in equations 11a–d, is the consequence of a discrete Wiener process.) Equations 11c and d are implicit due to the presence of the $\mathbf{v}_{ij}(t+\Delta t)$ terms on the right side of each equation. However, they can be rewritten in an explicit form (*18*) that eliminates these terms, which are then given as:

$$\mathbf{p}_i(t+\Delta t)=\mathbf{p}_i\left(t+\frac{\Delta t}{2}\right)-\frac{\Delta t}{2}\frac{\gamma_{ij}\omega^D}{1+\frac{\mu_{ij}}{2}\gamma_{ij}\omega^D\Delta t}\left\{\left[\frac{\mathbf{r}_{ij}}{r_{ij}}\cdot\mathbf{v}_{ij}\left(t+\frac{\Delta t}{2}\right)\right]\frac{\mathbf{r}_{ij}}{r_{ij}}+\sqrt{\Delta t}\,\frac{\mu_{ij}}{2}\sigma_{ij}\omega^R\varsigma_{ij}\frac{\mathbf{r}_{ij}}{r_{ij}}\right\}$$
$$+\frac{\sqrt{\Delta t}}{2}\sigma_{ij}\omega^R\varsigma_{ij}\frac{\mathbf{r}_{ij}}{r_{ij}}, \tag{11e}$$

and

$$\mathbf{p}_j(t+\Delta t)=\mathbf{p}_j\left(t+\frac{\Delta t}{2}\right)+\frac{\Delta t}{2}\frac{\gamma_{ij}\omega^D}{1+\frac{\mu_{ij}}{2}\gamma_{ij}\omega^D\Delta t}\left\{\left[\frac{\mathbf{r}_{ij}}{r_{ij}}\cdot\mathbf{v}_{ij}\left(t+\frac{\Delta t}{2}\right)\right]\frac{\mathbf{r}_{ij}}{r_{ij}}+\sqrt{\Delta t}\,\frac{\mu_{ij}}{2}\sigma_{ij}\omega^R\varsigma_{ij}\frac{\mathbf{r}_{ij}}{r_{ij}}\right\}$$
$$-\frac{\sqrt{\Delta t}}{2}\sigma_{ij}\omega^R\varsigma_{ij}\frac{\mathbf{r}_{ij}}{r_{ij}}, \tag{11f}$$

where $\mu_{ij}=\frac{1}{m_i}+\frac{1}{m_j}$.

As an alternative to the SSA formulation that determines the fluctuation-dissipation terms using a velocity-Verlet algorithm, here we also provide a modified SSA, where the velocity-Verlet algorithm is replaced by an implicit algorithm based upon the following arguments. For conservative systems, the Liouville equation indicates that the flow of system points in phase-space is incompressible. The velocity-Verlet algorithm is reversible and area-preserving, and thus possesses this desirable property for molecular dynamics simulations (*29–32*). However, DPD incorporates dissipative and random forces such that the volume element in phase-space is not preserved and the trajectories are not time-reversible. Moreover, the motion of the density of system points in phase-space is a Fokker-Planck (diffusion) equation, leading to a physical increase of the phase-space volume as the diffusive dynamics irreversibly evolves. Therefore, ensuring time reversibility of the integration of $\phi^{diss}_{\Delta t;i,j}$ is not necessary. Consequently, we propose the following implicit algorithm as an alternative to the velocity-Verlet algorithm to integrate this contribution:

$$\mathbf{p}_i(t+\Delta t)=\mathbf{p}_i(t)-\Delta t\gamma_{ij}\omega^D\left[\frac{\mathbf{r}_{ij}}{r_{ij}}\cdot\mathbf{v}_{ij}(t+\Delta t)\right]\frac{\mathbf{r}_{ij}}{r_{ij}}+\sqrt{\Delta t}\sigma_{ij}\omega^R\varsigma_{ij}\frac{\mathbf{r}_{ij}}{r_{ij}} \tag{11g}$$

and

$$\mathbf{p}_j(t+\Delta t)=\mathbf{p}_j(t)+\Delta t\gamma_{ij}\omega^D\left[\frac{\mathbf{r}_{ij}}{r_{ij}}\cdot\mathbf{v}_{ij}(t+\Delta t)\right]\frac{\mathbf{r}_{ij}}{r_{ij}}-\sqrt{\Delta t}\sigma_{ij}\omega^R\varsigma_{ij}\frac{\mathbf{r}_{ij}}{r_{ij}}. \tag{11h}$$

Analogous to the derivation of equations 11e and 11f, equations 11g and 11h can be rewritten in an explicit form as:

$$\mathbf{p}_i(t+\Delta t)=\mathbf{p}_i(t)-\frac{\gamma_{ij}\omega^D\Delta t}{1+\mu_{ij}\gamma_{ij}\omega^D\Delta t}\left\{\left[\frac{\mathbf{r}_{ij}}{r_{ij}}\cdot\mathbf{v}_{ij}(t)\right]\frac{\mathbf{r}_{ij}}{r_{ij}}+\mu_{ij}\sigma_{ij}\omega^R\varsigma_{ij}\frac{\mathbf{r}_{ij}}{r_{ij}}\sqrt{\Delta t}\right\}+\sqrt{\Delta t}\sigma_{ij}\omega^R\varsigma_{ij}\frac{\mathbf{r}_{ij}}{r_{ij}} \tag{11i}$$

and

$$\mathbf{p}_j(t+\Delta t)=\mathbf{p}_j(t)+\frac{\gamma_{ij}\omega^D\Delta t}{1+\mu_{ij}\gamma_{ij}\omega^D\Delta t}\left\{\left[\frac{\mathbf{r}_{ij}}{r_{ij}}\cdot\mathbf{v}_{ij}(t)\right]\frac{\mathbf{r}_{ij}}{r_{ij}}+\mu_{ij}\sigma_{ij}\omega^R\varsigma_{ij}\frac{\mathbf{r}_{ij}}{r_{ij}}\sqrt{\Delta t}\right\}-\sqrt{\Delta t}\sigma_{ij}\omega^R\varsigma_{ij}\frac{\mathbf{r}_{ij}}{r_{ij}}. \tag{11j}$$

Finally, the conservative term $\phi^C_{\Delta t}$ is approximated using the velocity-Verlet algorithm, where the momenta and positions are updated as

$$\mathbf{p}_i\left(t+\frac{\Delta t}{2}\right)=\mathbf{p}_i(t)+\frac{\Delta t}{2}\mathbf{F}_i^C(t)$$

$$\mathbf{r}_i(t+\Delta t)=\mathbf{r}_i(t)+\Delta t\frac{\mathbf{p}_i\left(t+\frac{\Delta t}{2}\right)}{m_i} \qquad (i=1,\ldots,N) \tag{12}$$

$$\text{evaluate} \quad \left\{\mathbf{F}_i^C(t+\Delta t)\right\}_{i=1}^N$$

$$\mathbf{p}_i(t+\Delta t)=\mathbf{p}_i\left(t+\frac{\Delta t}{2}\right)+\frac{\Delta t}{2}\mathbf{F}_i^C(t+\Delta t) \quad (i=1,\ldots,N)$$

We denote the original SSA given by equation 10, equations 11a, 11b, 11e, 11f, and 12 as SSA-VV, while the modified SSA given by equation 10, equations 11i and 11j, and equation 12 as SSA-I. The following outlines summarize the SSA-VV and SSA-I in a practical form. By comparing these forms, it is evident that the SSA-I requires fewer mathematical operations than the SSA-VV and thus is less computationally intensive. However, as demonstrated in section IV, the SSA-VV is a better performing integration scheme. Finally, note that for the proposed splitting schemes in the limit of vanishing dissipative and random forces, the reversibility of the trajectories and the area-preserving property is recovered, as expected.

(I) Outline of the SSA-VV for constant-temperature DPD:

1. *Stochastic Integration* for all $i-j$ pairs of particles:

   (a) $\mathbf{p}_i \leftarrow \mathbf{p}_i-\frac{\Delta t}{2}\gamma_{ij}\omega^D\left(\frac{\mathbf{r}_{ij}}{r_{ij}}\cdot\mathbf{v}_{ij}\right)\frac{\mathbf{r}_{ij}}{r_{ij}}+\sigma_{ij}\omega^R\zeta_{ij}\frac{\mathbf{r}_{ij}}{r_{ij}}\frac{\sqrt{\Delta t}}{2}$

   (b) $\mathbf{p}_j \leftarrow \mathbf{p}_j+\frac{\Delta t}{2}\gamma_{ij}\omega^D\left(\frac{\mathbf{r}_{ij}}{r_{ij}}\cdot\mathbf{v}_{ij}\right)\frac{\mathbf{r}_{ij}}{r_{ij}}-\sigma_{ij}\omega^R\zeta_{ij}\frac{\mathbf{r}_{ij}}{r_{ij}}\frac{\sqrt{\Delta t}}{2}$

   (c) $\mathbf{v}_{ij} \leftarrow \frac{\mathbf{p}_i}{m_i}-\frac{\mathbf{p}_j}{m_j}$

   (d) $\mathbf{p}_i \leftarrow \mathbf{p}_i-\frac{\Delta t}{2}\frac{\gamma_{ij}\omega^D}{1+\frac{\mu_{ij}}{2}\gamma_{ij}\omega^D\Delta t}\left[\left(\frac{\mathbf{r}_{ij}}{r_{ij}}\cdot\mathbf{v}_{ij}\right)\frac{\mathbf{r}_{ij}}{r_{ij}}+\frac{\mu_{ij}}{2}\sigma_{ij}\omega^R\zeta_{ij}\frac{\mathbf{r}_{ij}}{r_{ij}}\sqrt{\Delta t}\right]+\sigma_{ij}\omega^R\zeta_{ij}\frac{\mathbf{r}_{ij}}{r_{ij}}\frac{\sqrt{\Delta t}}{2}$

   (e) $\mathbf{p}_j \leftarrow \mathbf{p}_j+\frac{\Delta t}{2}\frac{\gamma_{ij}\omega^D}{1+\frac{\mu_{ij}}{2}\gamma_{ij}\omega^D\Delta t}\left[\left(\frac{\mathbf{r}_{ij}}{r_{ij}}\cdot\mathbf{v}_{ij}\right)\frac{\mathbf{r}_{ij}}{r_{ij}}+\frac{\mu_{ij}}{2}\sigma_{ij}\omega^R\zeta_{ij}\frac{\mathbf{r}_{ij}}{r_{ij}}\sqrt{\Delta t}\right]-\sigma_{ij}\omega^R\zeta_{ij}\frac{\mathbf{r}_{ij}}{r_{ij}}\frac{\sqrt{\Delta t}}{2}$

2. *Deterministic Integration no. 1* for $i=1,\ldots,N$:

   (a) $\mathbf{p}_i \leftarrow \mathbf{p}_i+\frac{\Delta t}{2}\mathbf{F}_i^C$

   (b) $\mathbf{r}_i \leftarrow \mathbf{r}_i+\Delta t\frac{\mathbf{p}_i}{m_i}$

3. *Conservative Force Calculation*: $\left\{\mathbf{F}_i^C\right\}_{i=1}^N$
4. *Deterministic Integration no. 2* for $i = 1,...,N$:

$$\mathbf{p}_i \leftarrow \mathbf{p}_i + \frac{\Delta t}{2}\mathbf{F}_i^C$$

(II) Outline of the SSA-I for constant-temperature DPD:

1. *Stochastic Integration* for all $i - j$ pairs of particles:

(a) $$\mathbf{p}_i \leftarrow \mathbf{p}_i - \frac{\gamma_{ij}\omega^D\Delta t}{1+\mu_{ij}\gamma_{ij}\omega^D\Delta t}\left[\left(\frac{\mathbf{r}_{ij}}{r_{ij}}\cdot\mathbf{v}_{ij}\right)\frac{\mathbf{r}_{ij}}{r_{ij}} + \mu_{ij}\sigma_{ij}\omega^R\zeta_{ij}\frac{\mathbf{r}_{ij}}{r_{ij}}\sqrt{\Delta t}\right] + \sigma_{ij}\omega^R\zeta_{ij}\frac{\mathbf{r}_{ij}}{r_{ij}}\sqrt{\Delta t}$$

(b) $$\mathbf{p}_j \leftarrow \mathbf{p}_j + \frac{\gamma_{ij}\omega^D\Delta t}{1+\mu_{ij}\gamma_{ij}\omega^D\Delta t}\left[\left(\frac{\mathbf{r}_{ij}}{r_{ij}}\cdot\mathbf{v}_{ij}\right)\frac{\mathbf{r}_{ij}}{r_{ij}} + \mu_{ij}\sigma_{ij}\omega^R\zeta_{ij}\frac{\mathbf{r}_{ij}}{r_{ij}}\sqrt{\Delta t}\right] - \sigma_{ij}\omega^R\zeta_{ij}\frac{\mathbf{r}_{ij}}{r_{ij}}\sqrt{\Delta t}$$

2. *Deterministic Integration no. 1* for $i = 1,...,N$:

(a) $$\mathbf{p}_i \leftarrow \mathbf{p}_i + \frac{\Delta t}{2}\mathbf{F}_i^C$$

(b) $$\mathbf{r}_i \leftarrow \mathbf{r}_i + \Delta t\frac{\mathbf{p}_i}{m_i}$$

3. *Conservative Force Calculation*: $\left\{\mathbf{F}_i^C\right\}_{i=1}^N$
4. *Deterministic Integration no. 2* for $i = 1,...,N$:

$$\mathbf{p}_i \leftarrow \mathbf{p}_i + \frac{\Delta t}{2}\mathbf{F}_i^C$$

3. Computational Details

The SSA-VV and SSA-I for the constant-temperature DPD method were tested using the standard DPD fluid (*13*), where details of the conservative forces for this model are given in appendix B. Both a pure component case and an equimolar binary mixture were tested for the DPD fluid model, with system sizes of $N = 10125$. For these simulations, the following reduced units were used: r_c is the unit of length; the mass of a DPD particle is the unit of mass; and the unit of energy is $k_{\mathrm{B}}T$. Using these reduced units, we set the maximum repulsion between particles i and j as $a_{ij} = 25$ for the pure DPD fluid, and as $a_{ij} = 25$ and 28 for the like and unlike $i - j$ interactions, respectively, for the binary DPD fluid. Further, for all cases, we set the noise amplitude $\sigma_{ij} = 3$.

4. Results Comparison of SSA-VV and SSA-I Performance

For both the pure and equimolar binary DPD fluids, we performed constant-temperature DPD simulations at particle density $\rho = \frac{N}{V} = 3$ and $T = 1$ using the SSA-VV and SSA-I, where Δt was varied from 0.01 to 0.15. For the various time steps and runs of length $t_{run} = 5000$, figure 1 (pure fluid) and figure 2 (equimolar binary fluid) compare values of the simulated kinetic temperature $\langle T_{kin} \rangle = \left\langle \frac{1}{3k_B N} \sum_{i=1}^{N} \frac{\mathbf{p}_i \cdot \mathbf{p}_i}{m_i} \right\rangle$ to the prescribed T, along with the configurational energy per particle $\langle u \rangle$, and virial pressure $\langle P_{vir} \rangle$ ($\langle . \rangle$ denotes an ensemble average). Values of $(\langle T_{kin} \rangle - T)/T$, $\langle u \rangle$ and $\langle P_{vir} \rangle$ for Δt >0.07 begin to significantly diverge and therefore are not shown in figures 1 and 2. For both fluids, the SSA-I systematically underestimates T by approximately 1%–2% for Δt below 0.07, but more importantly its performance shows non-monotonic dependence on Δt, which is undesirable behavior for a numerical integrator. From a practical viewpoint, figures 1 and 2, and the values of other properties such as the radial distribution function and self-diffusion coefficient (not shown here), suggest that for all values of $\Delta t \leq 0.05$, the results of the constant-temperature DPD simulations are within good agreement for both the SSA-VV and SSA-I.

For completeness, also shown in figures 1 and 2 is the standard velocity-Verlet (SVV) algorithm (*13*) often used for DPD simulations. Comparing the SSA-VV and SVV, we see that $(\langle T_{kin} \rangle - T)/T$ is positive and increases with increasing Δt for both algorithms. However, the SSA-VV is superior in comparison with the SVV for both the pure (in agreement with previous work [*18*]) and binary DPD fluids.

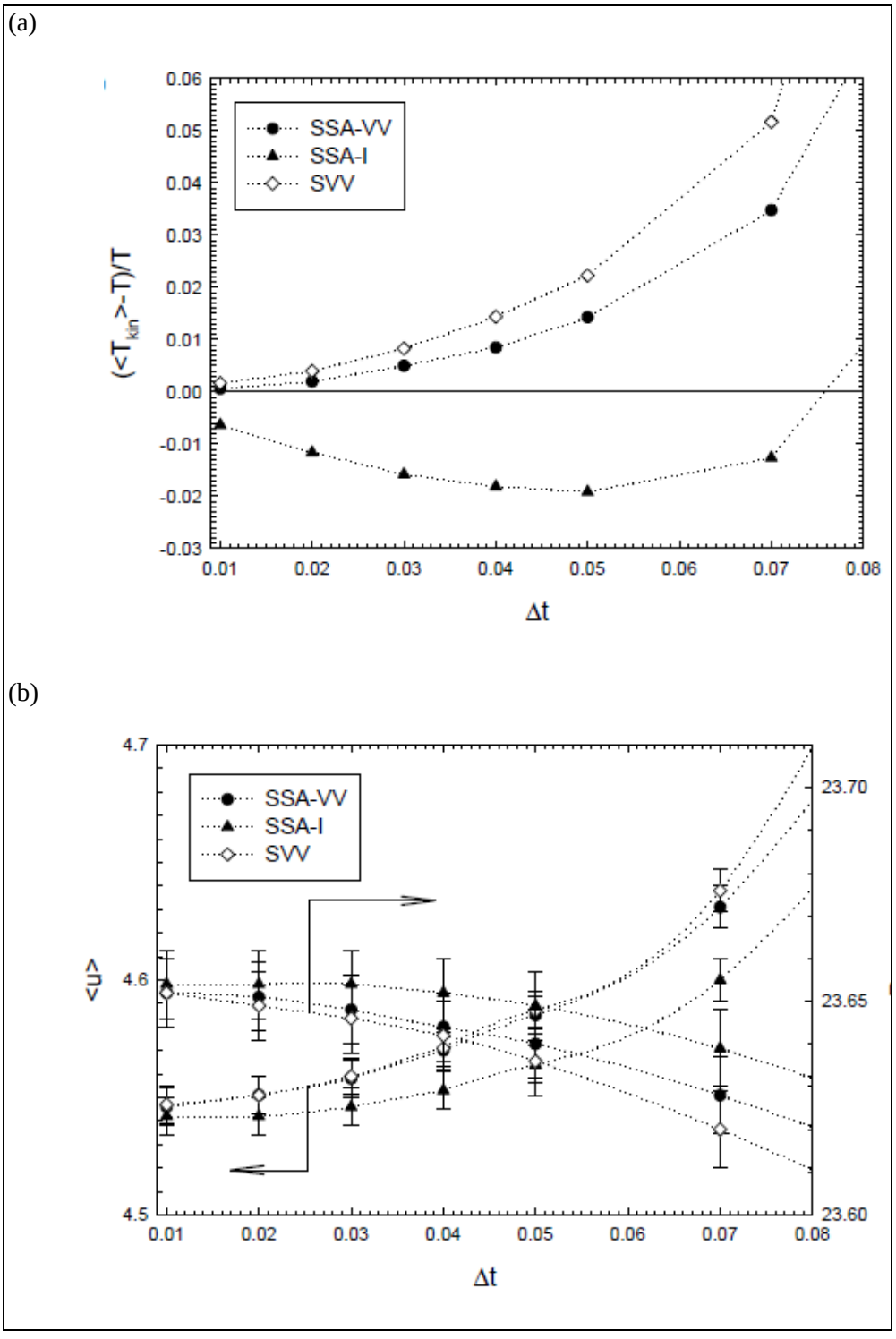

Figure 1. (a) The simulated kinetic temperature $\langle T_{kin} \rangle$ and (b) the configurational energy per particle $\langle u \rangle$ and the virial pressure $\langle P_{vir} \rangle$ of the pure DPD fluid as a function of the integration time step Δt for constant-temperature DPD simulations with the SSA-VV, SSA-I, and SVV integrators at $\rho = 3$ and $T = 1$.

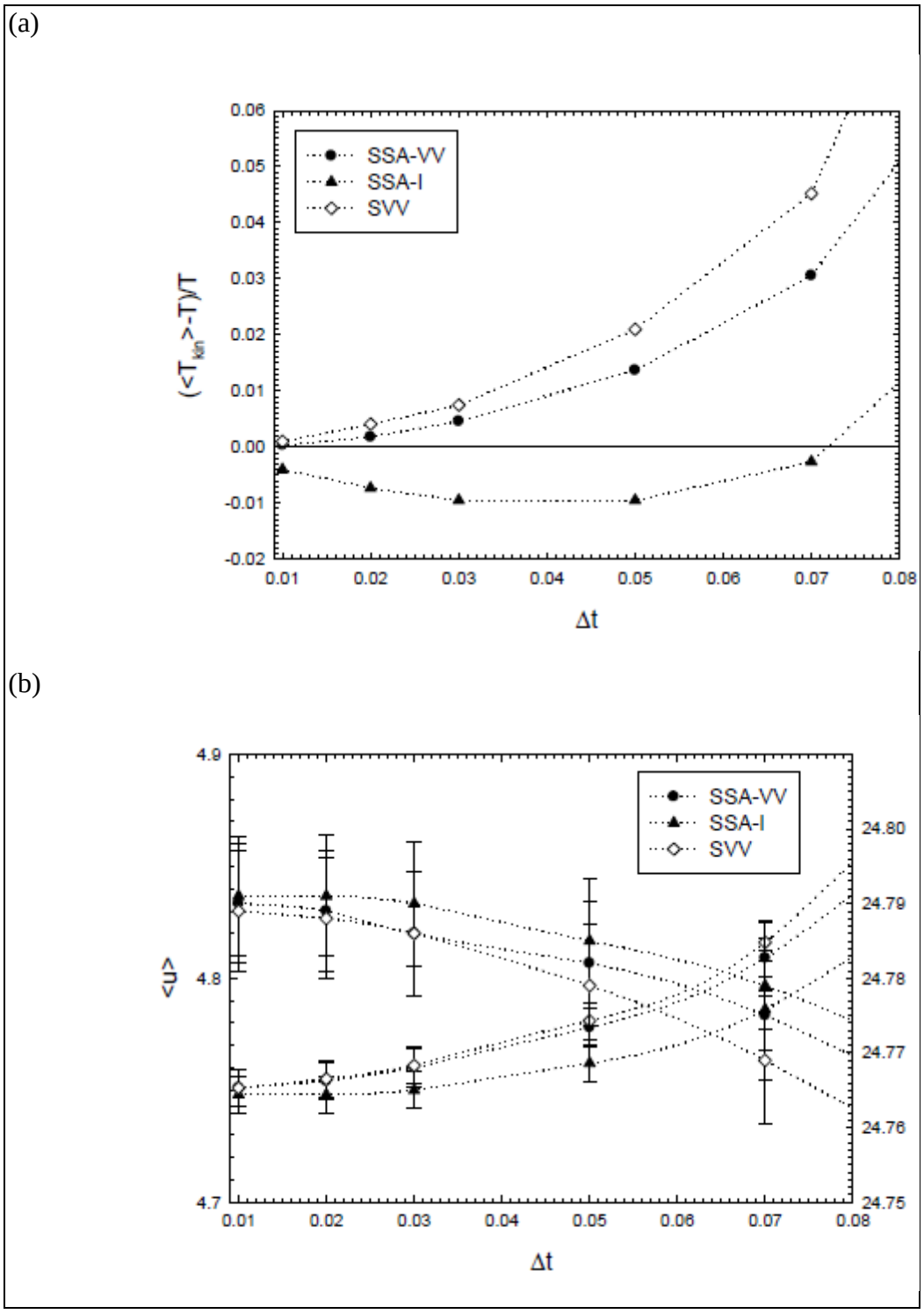

Figure 2. (a) The simulated kinetic temperature $\langle T_{kin} \rangle$ and (b) the configurational energy per particle $\langle u \rangle$ and the virial pressure $\langle P_{vir} \rangle$ of the equimolar binary DPD fluid as a function of the integration time step Δt for constant-temperature DPD simulations with the SSA-VV, SSA-I, and SVV integrators at $\rho = 3$ and $T = 1$.

5. Conclusion

A comprehensive description of numerical integration schemes based upon the Shardlow-splitting algorithm was presented for the constant-temperature DPD method. The original SSA formulated for systems of equal-mass particles has been extended to systems of unequal-mass particles. Both a velocity-Verlet scheme and an implicit scheme were formulated for the integration of the fluctuation-dissipation contribution, where the velocity-Verlet scheme consistently performed better.

6. References

1. Hoogerbrugge, P. J.; Koelman, J. M. V. A. Simulating Microscopic Hydrodynamic Phenomena With Dissipative Particle Dynamics. *Europhys. Lett*. **1992**, *19*, 155.
2. Koelman, J. M. V. A.; Hoogerbrugge, P. J., Dynamic Simulation of Hard Sphere Suspensions Under Steady Shear. *Europhys. Lett*. **1993**, *21*, 363.
3. Brennan, J. K.; Lísal, M. Dissipative Particle Dynamics: Addressing Deficiencies and Establishing New Frontiers. *Molec. Simul*. **2009**, *35*, 766.
4. Venturoli, M.; Sperotto, M. M.; Kranenburg, M.; Smit., B. Mesoscopic Models of Biological Membranes. *Phys. Rep*. **2006**, *437*, 1.
5. Stoltz, G. A Reduced Model for Shock and Detonation Waves: I. The Inert Case. *Europhys. Lett*. **2006**, *76*, 849.
6. Pagonabarraga, I.; Frenkel, D. Dissipative Particle Dynamics for Interacting Systems. *J. Chem. Phys*. **2001**, *115*, 5015.
7. Pan, W.; Caswell, B.; Karniadakis, G. E. Rheology, Microstructure and Migration in Brownian Colloidal Suspensions. *Langmuir* **2009**, *26*, 133.
8. Brennan, J. K.; Lísal, M. Coarse-Grain Models for Metals: Constant-Pressure Dissipative Dynamics Simulations. *Proceedings of the 14th International Detonation Symposium Office of Naval Research*, Coeur d'Alene, ID, 11–16 April, 2010; p 1451.
9. Whittle, M.; Travis, K. P. Dynamic Simulations of Colloids by Core-Modified Dissipative Particle Dynamics. *J. Chem. Phys*. **2010**, *132*, 124906.
10. Groot, R. D.; Stoyanov, S. D. Mesoscopic Model for Colloidal Particles, Powders, and Granular Solids. *Phys. Rev. E* **2008**, *78*, 051403.
11. Nikunen, P.; Karttunen, M.; Vattulainen, I. How Would You Integrate the Equations of Motion in Dissipative Particle Dynamics Simulations? *Comp. Phys. Comm*. **2003**, *153*, 407.
12. Chaudhri, A.; Lukes, J. R. Velocity and Stress Autocorrelation Decay in Isothermal Dissipative Particle Dynamics. *Phys. Rev. E* **2010**, *81*, 026707.
13. Groot, R. D.; Warren, P. B. Dissipative Particle Dynamics: Bridging the Gap Between Atomistic and Mesoscopic Simulation. *J. Chem. Phys*. **1997**, *107*, 4423.
14. Pagonabarraga, I.; Hagen, M. H. J.; Frenkel, D. Self-Consistent Dissipative Particle Dynamics Algorithm. *Europhys. Lett*. **1998**, *42*, 377.

15. Besold, G.; Vattulainen, I.; Karttunen, M.; Polson, J. M. Towards Better Integrators for Dissipative Particle Dynamics Simulations. *Phys. Rev. E.* **2000**, *62*, R7611.

16. Vattulainen, I.; Karttunen, M.; Besold, G.; Polson, J. M. Integration Schemes for Dissipative Particle Dynamics Simulations: From Softly Interacting Systems Towards Hybrid Models. *J. Chem. Phys.* **2002**, *116*, 3967.

17. den Otter, W. K.; Clarke, J. H. R. A New Algorithm for Dissipative Particle Dynamics. *Europhys. Lett.* **2001**, *53*, 426.

18. Shardlow, T. Splitting for Dissipative Particle Dynamics. *SIAM J. Sci. Comput*. **2003**, *24*, 1267.

19. Lowe, C. P. An Alternative Approach to Dissipative Particle Dynamics. *Europhys. Lett.* **1999**, *47*, 145.

20. Peters, E. A. J. F. Elimination of Time Step Effects in DPD. *Europhys. Lett*. **2004**, *66*, 311.

21. Litvinov, S.; Ellero, M.; Hu, X. Y.; Adams, N. A. A Splitting Scheme for Highly Dissipative Smoothed Particle Dynamics. *J. Comput. Phys*. **2010**, *229*, 5457.

22. De Fabritiis, G.; Serrano, M.; Español, P.; Coveney, P. V. Efficient Numerical Integrators for Sochastic Models. *Physica A* **2006**, *361*, 429.

23. Serrano, M.; De Fabritiis, G.; Español P.; Coveney, P. V. A Stochastic Trotter Integration Scheme for Dissipative Particle Dynamics. *Math. Comput. Simul*. **2006**, *72*, 190.

24. Merabia, S.; Bonet Avalos, J. Dewetting of a Stratified Two-Component Liquid Film on a Solid Substrate. *Phys. Rev. Lett*. **2008**, *101*, 208303.

25. Risken, H. *The Fokker-Planck Equation*; Springer-Verlag: Berlin, 1996.

26. Gardiner, C. W. *Handbook of Stochastic Methods*; Springer-Verlag: Berlin, 2004.

27. Español, P.; Warren, P. B. Statistical Mechanics of Dissipative Particle Dynamics. *Europhys. Lett*. 1995, *30*, 191.

28. Allen, M. P.; Tildesley, D. J. *Computer Simulation of Liquids*; Clarendon Press: Oxford, UK, 1987.

29. Frenkel, D.; Smit, B. *Understanding Molecular Simulation: From Algorithms to Applications*; Academic Press: London, UK, 2002.

30. Tuckerman, M. E.; Berne, B. J.; Martyna, G. J. Reversible Multiple Time Scale Molecular Dynamics. *J. Chem. Phys*. **1992**, *97*, 1990.

31. Hairer, E.; Lubich, C.; Wanner, G. *Geometric Numerical Integration: Structure-Preserving Algorithms for Ordinary Differential Equations*; Springer-Verlag: Berlin, 2006.

32. Leimkuhler, B.; Reich, S. *Simulating Hamiltonian Dynamics*; Cambridge University Press: Cambridge, MA, 2004.

INTENTIONALLY LEFT BLANK.

Appendix A. Fokker-Planck Equation (FPE) and Fluctuation-Dissipation Theorem (FDT)

The Fokker-Planck equation (FPE) corresponding to the equations of motion given by equations 5a and 5b of this report is

$$\frac{\partial \rho}{\partial t} = L_C \rho + L_D \rho , \tag{A-1}$$

where $\rho \equiv \rho(\mathbf{r},\mathbf{p};t)$ is the time-dependent probability density, $\mathbf{r} \equiv \{\mathbf{r}_i\}_{i=1}^N$ and $\mathbf{p} \equiv \{\mathbf{p}_i\}_{i=1}^N$ are particle positions and momenta, respectively, and N is the total number of particles. In equation A-1, we have defined the operators

$$L_C \equiv -\left(\sum_i \frac{\mathbf{p}_i}{m_i} \cdot \frac{\partial}{\partial \mathbf{r}_i} + \sum_i \sum_{j \neq i} \mathbf{F}_{ij}^C \cdot \frac{\partial}{\partial \mathbf{p}_i} \right) \tag{A-2}$$

and

$$L_D \equiv \sum_i \sum_{j \neq i} \frac{\mathbf{r}_{ij}}{r_{ij}} \cdot \frac{\partial}{\partial \mathbf{p}_i} \left[\gamma_{ij} \omega^D \left(\frac{\mathbf{r}_{ij}}{r_{ij}} \cdot \mathbf{v}_{ij} \right) + \frac{\sigma_{ij}^2}{2} \left(\omega^R \right)^2 \left(\frac{\partial}{\partial \mathbf{p}_i} - \frac{\partial}{\partial \mathbf{p}_j} \right) \cdot \frac{\mathbf{r}_{ij}}{r_{ij}} \right], \tag{A-3}$$

where m_i is the mass of particle i, $\mathbf{r}_{ij} = \mathbf{r}_i - \mathbf{r}_j$ is the separation vector between particle i and particle j, $r_{ij} = \left| \mathbf{r}_{ij} \right|$, $\mathbf{F}_{ij}^C$ is the conservative force acting between particle i and particle j, γ_{ij} and σ_{ij} are the friction coefficient and noise amplitude between particle i and particle j, respectively, $\mathbf{v}_{ij} = \frac{\mathbf{p}_i}{m_i} - \frac{\mathbf{p}_j}{m_j}$, and ω^D and ω^R are weight functions of the dissipative and random forces, respectively. L_C is the Liouville operator corresponding to a Hamiltonian system interacting with conservative forces $\mathbf{F}^C$. The operator L_D takes into account the effects of the dissipative and random forces.

The equilibrium probability density $\rho^{eq} \equiv \rho^{eq}(\mathbf{r},\mathbf{p})$ should be a steady-state solution of the FPE, $\frac{\partial \rho}{\partial t} = 0$. Thus, the FDT can be derived by imposing that ρ^{eq} corresponds to the canonical (Gibbs-Boltzmann) probability density:

$$\begin{aligned} \rho^{eq}(\mathbf{r},\mathbf{p}) &= \frac{1}{Z} \exp\left[-\frac{H(\mathbf{r},\mathbf{p})}{k_B T} \right] \\ &= \frac{1}{Z} \exp\left(-\frac{\sum_i \frac{\mathbf{p}_i \cdot \mathbf{p}_i}{2m_i} + \sum_i \sum_{j>i} u_{ij}^{CG}}{k_B T} \right), \end{aligned} \tag{A-4}$$

where $H(\mathbf{r},\mathbf{p})$ is the Hamiltonian of a dissipative particle dynamics (DPD) system, Z is the normalizing partition function, k_{B} is the Boltzmann constant, T is the system temperature, and u_{ij}^{CG} is a coarse-grain potential. $L_C\rho^{eq}=0$ since the canonical probability density is the equilibrium solution for the conservative system. The FDT then follows from the requirement $L_D\rho^{eq}=0$, which is satisfied for

$$\sigma_{ij}^2\left(\omega^R\right)^2 = 2\gamma_{ij}\omega^D k_{\mathrm{B}}T\,,$$

i.e., for

$$\begin{aligned}\sigma_{ij}^2 &= 2\gamma_{ij}k_{\mathrm{B}}T\\ \left(\omega^R\right)^2 &= \omega^D\end{aligned}\,. \qquad \text{(A-5)}$$

The physical interpretation of the FDT, equation A-5, is the following. In a constant-temperature DPD simulation, the system is implicitly connected to a heat reservoir whose temperature corresponds to the imposed temperature. During the simulation, heat is exchanged between the heat reservoir and the system such that the average temperature of the system equals the reservoir temperature. Thus, the FDT indicates that the amplitude of the random-force friction coefficient σ_{ij} depends upon the system temperature.

INTENTIONALLY LEFT BLANK.

Appendix B. Simulation Model Details

For the models considered in this work, the details of the conservative forces expressed in equation 2 of the main text are the following: u_{ij}^{CG} for the pure and binary dissipative particle dynamics fluids[1] is given by

$$u_{ij}^{CG} = a_{ij} r_c \omega^D \left(r_{ij} \right) \tag{B-1}$$

where a_{ij} is the maximum repulsion between particle i and particle j.

[1]Groot, R. D.; Warren, P. B. Dissipative Particle Dynamics: Bridging the Gap Between Atomistic and Mesoscopic Simulation. *J. Chem. Phys*. **1997**, *107*, 4423.

List of Symbols, Abbreviations, and Acronyms

DPD	dissipative particle dynamics
EOM	equations-of-motion
FPE	Fokker-Planck equation
FDT	fluctuation-dissipation theorem
SDEs	stochastic differential equations
SSA	Shardlow-splitting algorithm
SSA-VV	Shardlow-splitting algorithm-velocity Verlet
SSA-I	Shardlow-splitting algorithm-implicit
SVV	standard velocity-Verlet

NO. OF
COPIES ORGANIZATION

1 (PDF) DEFENSE TECHNICAL INFORMATION CTR DTIC OCA

1 (PDF) DIRECTOR US ARMY RESEARCH LAB IMAL HRA

1 (PDF) DIRECTOR US ARMY RESEARCH LAB RDRL CIO LL

1 (PDF) GOVT PRINTG OFC A MALHOTRA

ABERDEEN PROVING GROUND

1 (PDF) DIR USARL RDRL WML B J BRENNAN